

Temporal Leakage in Analysis of Electromagnetic Systems

Djordjević, A.R., Tosić, D.V., Zajić, A.G.; Nikolić, M.M.; Olcan, D.I.; Jovanović, I.D.
Sch. of Electr. Eng., Univ. of Belgrade, Belgrade, Serbia

© 2012 IEEE. Personal use of this material is permitted. Permission from IEEE must be obtained for all other uses, in any current or future media, including reprinting/republishing this material for advertising or promotional purposes, creating new collective works, for resale or redistribution to servers or lists, or reuse of any copyrighted component of this work in other works.

Abstract available at: <http://ieeexplore.ieee.org/xpl/articleDetails.jsp?reload=true&arnumber=6387785>

This paper appears in: [Antennas and Propagation Magazine, IEEE](#)

Date of Publication: December 2012

Volume: 54, **Issue:** 6

Page(s): 92 - 101

ISSN: 1045-9243

DOI: [10.1109/MAP.2012.6387785](https://doi.org/10.1109/MAP.2012.6387785)

Date of Current Version: 20 December 2012

Temporal Leakage in Analysis of Electromagnetic Systems

Antonije R. Djordjević¹, Dejan V. Tošić¹, Alenka G. Zajić², *Member, IEEE*, Marija M. Nikolić¹, Dragan I. Olčan¹, *Member, IEEE*, and Izabela D. Jovanović³

¹School of Electrical Engineering, University of Belgrade

King Alexander's Boulevard 73, 11120 Belgrade, Serbia

Tel: +381 11 3218 329; Fax: +381 11 3248 681; E-mails: edjordja@etf.rs, tosic@etf.rs, mnikolic@etf.rs,
olcan@etf.rs

²School of Computer Science, Georgia Institute of Technology, 266 Ferst Dr, Atlanta, GA 30332-0765,
USA

Tel: +1 404 385-6604; E-mail: azajic@cc.gatech.edu

³Telekom Srbija, Katićeva 14, 11000 Belgrade, Serbia

Tel: +381 11 3069 723; Fax: +381 11 3628 015; E-mail izabela@telekom.rs

Abstract

Temporal leakage occurs when the time-domain response of a linear electromagnetic system is computed from frequency-domain data using the inverse discrete Fourier transform. Although the temporal leakage occurs in most practical cases, this phenomenon is not recognized in the literature covering electromagnetics, antennas, and microwaves. The purpose of the paper is to demonstrate and explain the temporal leakage.

Keywords: Discrete Fourier transform, computational electromagnetics, time-domain response, temporal leakage

1. Introduction

Various linear time-invariant electromagnetic systems are most conveniently analyzed in the frequency domain because there exist mature computational techniques (e.g., [1]) and related software (e.g., [2, 3]). Also, most measurements of antenna and microwave systems are performed in the frequency domain (using vector network analyzers), yielding a discrete set of frequency-domain data. In order to obtain the time-domain response of such systems, the inverse discrete Fourier transform (inverse DFT) is often used (e.g., [4]), which is implemented as a fast Fourier transform (FFT) algorithm. In the application of the DFT, an apparently noncausal response can be obtained in the time domain, in spite of careful modeling in the frequency domain or carefully calibrated measurements. This unexpected response appears in the form of fast oscillations that occur before a sharp edge of the physically meaningful time-domain response.

The same problem also occurs in the analysis of electrical circuits. An example is shown in Fig. 7 of [5], where the noncausal oscillations are mistakenly attributed to the Gibbs phenomenon. However, the problem is actually associated with an inherent feature of the DFT, which is referred to as the “temporal leakage” [6-11]. This phenomenon is mentioned only in very few references, away from the electromagnetic community, although its counterpart, the “spectral leakage”, is extensively elaborated in the literature (e.g., [12, 13]).

The purpose of this paper is to show some typical cases where the temporal leakage occurs in the electromagnetic analysis and measurements, and give mathematical explanation of the phenomenon. Consequently, in Section 2 the discrete Fourier transform is briefly revisited, in Section 3 the mathematical background of the temporal leakage is elaborated, and in Section 4 several examples are given illustrating this phenomenon.

2. Discrete Fourier Transform

The DFT can be introduced by considering a periodic sequence of equispaced Dirac’s delta-functions (impulses) in the time domain, $\delta(t)$, and *exactly* evaluating the corresponding Fourier transform, which is also a periodic sequence of equispaced impulses. The proof is given below. This approach is somewhat unusual, but it is useful for explaining the temporal leakage and some other peculiarities of the DFT.

Consider a sequence of N impulses in the time domain (temporal functions), at time instants $0, \Delta t, 2\Delta t, \dots, (N-1)\Delta t$, where Δt is the time step and $N\Delta t = T$. The amplitudes of the impulses are x_0, x_1, \dots, x_{N-1} . This sequence is periodically repeated with the period T . Mathematically, this sequence can be defined on the interval $0 \leq t < T$ as

$$x_{\delta T}(t) = \sum_{n=0}^{N-1} x_n \delta(t - n\Delta t), \quad (1)$$

and then it is periodically repeated using $x_{\delta}(t + lT) = x_{\delta T}(t)$, where l is an arbitrary integer. Alternatively, we can write

$$x_{\delta}(t) = \sum_{n=-\infty}^{+\infty} x_n \delta(t - n\Delta t), \quad x_{n+lN} = x_n. \quad (2)$$

The sequence $x_{\delta}(t)$ can also be represented in terms of the comb function, as follows. The comb function is a periodic train of impulses, with the period T :

$$\Delta_T(t) = \sum_{m=-\infty}^{+\infty} \delta(t - mT). \quad (3)$$

The function $x_{\delta}(t)$ can be expressed as a sum of interleaved comb functions, which are shifted for $n\Delta t$, $n = 0, \dots, N - 1$, as

$$x_{\delta}(t) = \sum_{n=0}^{N-1} x_n \Delta_T(t - n\Delta t), \quad (4)$$

where each comb function is multiplied (weighted) by x_n .

We now evaluate the Fourier transform (Fourier integral) of $x_{\delta}(t)$. Since $\Delta_T(t)$ is a periodic function, it can be expanded in the Fourier series. The coefficients of the series are $c_k = \frac{1}{T} \int_{-T/2}^{T/2} \delta(t) e^{\frac{2\pi jkt}{T}} dt = \frac{1}{T}$, where

k is an integer, $k \in (-\infty, +\infty)$, and j is the imaginary unit, so that $\Delta_T(t) = \frac{1}{T} \sum_{k=-\infty}^{+\infty} e^{\frac{2\pi jkt}{T}}$. On the other hand, the

Fourier transform of $e^{\frac{2\pi jkt}{T}}$ is $\delta\left(f - \frac{k}{T}\right)$. Hence, the Fourier transform of $\Delta_T(t)$ is

$$\frac{1}{T} \sum_{k=-\infty}^{+\infty} \delta\left(f - \frac{k}{T}\right) = \Delta f \sum_{k=-\infty}^{+\infty} \delta(f - k\Delta f) = \Delta f \Delta_{\Delta f}(f), \quad (5)$$

where $\Delta f = \frac{1}{T}$. It is also a comb of delta-functions, but in the spectral (frequency) domain, with the spectral-domain period Δf .

The Fourier transform of each comb function in (4) can be obtained from (5) by using the shift theorem, i.e., it is given by $\Delta f \Delta_{\Delta f}(f) e^{-2\pi jfn\Delta t} = \Delta f \sum_{k=-\infty}^{+\infty} \delta(f - k\Delta f) e^{-2\pi jfn\Delta t} = \Delta f \sum_{n=-\infty}^{+\infty} \delta(f - k\Delta f) e^{-2\pi j \frac{kn}{N}}$ because

$\delta(f)g(f) = \delta(f)g(0)$, where $g(f)$ is an arbitrary function defined at $f = 0$ and continuous at $f = 0$, and $e^{-2\pi jk\Delta f n \Delta t} = e^{-2\pi j \frac{kn}{N}}$, because $\Delta t \Delta f = \frac{1}{N}$.

By summing the Fourier transforms for all comb functions, a sequence of weighted delta-functions in the spectral domain is obtained. Thereby, each delta-function is multiplied by $X_k = \frac{1}{T} \sum_{n=0}^{N-1} x_n e^{-2\pi j \frac{kn}{N}} = \Delta f \sum_{n=0}^{N-1} x_n e^{-2\pi j \frac{kn}{N}}$, $k \in (-\infty, +\infty)$. Since n is an integer, we have $e^{-2\pi j \frac{(k+N)n}{N}} = e^{-2\pi j \frac{kn}{N}}$, so that X_k is a periodic sequence of complex numbers, with the basic period N . Hence, it is sufficient to consider X_k only on the basic period, i.e., for $k = 0, \dots, N-1$, in the same way as it is sufficient to consider x_n only for $n = 0, 1, \dots, N-1$.

$$\text{Following a similar derivation, we can show that } x_n = \Delta t \sum_{k=0}^{N-1} X_k e^{2\pi j \frac{nk}{N}} = \frac{1}{N \Delta f} \sum_{k=0}^{N-1} X_k e^{2\pi j \frac{nk}{N}}.$$

Hence, we have obtained formulas for the physical (denormalized) discrete Fourier transform (DFT) and the corresponding inverse discrete Fourier transform (IDFT):

$$X_k = \Delta f \sum_{n=0}^{N-1} x_n e^{-2\pi j \frac{kn}{N}}, \quad k = 0, 1, \dots, N-1, \tag{6}$$

$$x_n = \frac{1}{N \Delta f} \sum_{k=0}^{N-1} X_k e^{2\pi j \frac{nk}{N}}, \quad n = 0, 1, \dots, N-1. \tag{7}$$

These transforms relate the amplitudes of a periodic sequence of impulses in the time domain (x_n) to the amplitudes of a periodic sequence of impulses in the frequency domain (X_k). Note that relations (6) and (7) are *exact*, and that the sequences of pulses in both domains are infinite and periodic.

The normalized forms of the DFT and IDFT are obtained by artificially taking $\Delta f = 1$ (also neglecting the units), so that

$$X_k = \sum_{n=0}^{N-1} x_n e^{-2\pi j \frac{kn}{N}}, \quad k = 0, 1, \dots, N-1, \tag{8a}$$

$$x_n = \frac{1}{N} \sum_{k=0}^{N-1} X_k e^{2\pi j \frac{nk}{N}}, \quad k = 0, 1, \dots, N-1. \tag{8b}$$

The normalized forms are practically the only ones found in the literature, and the available FFT algorithms are based on (8a) and (8b). From now on in this paper, we consider only the normalized forms.

If (1) represents a physical time-domain signal, then the amplitudes x_0, x_1, \dots, x_{N-1} are real numbers. The corresponding spectrum has a conjugate symmetry. Hence, the infinite sequence of complex numbers

$\{X_k\}$ has a conjugate symmetry: $X_{-k} = X_k^*$ for any integer k . Assuming N to be even, due to the periodicity of $\{X_k\}$, this sequence on the basic period looks as follows:

$$\{X_0, X_1, \dots, X_{N/2-1}, X_{N/2}, X_{N/2+1}, \dots, X_{N-1}\} = \{X_0, X_1, \dots, X_{N/2-1}, X_{N/2}, X_{N/2-1}^*, \dots, X_1^*\}. \quad (9)$$

The terms $X_{N/2}$ and X_0 are purely real due to the conjugate symmetry of $\{X_k\}$. If N is odd, the middle (purely real) term in this sequence does not exist, but X_0 is still purely real.

Hence, when analyzing or measuring an electromagnetic system in the frequency domain and evaluating the time-domain response using the IDFT, one should properly define the sequence $\{X_k\}$ in (8b) in order to obtain real-valued elements of the sequence $\{x_n\}$. The first part of $\{X_k\}$ is taken from the computed or measured data, and the second part is defined based on the conjugate symmetry, as in (9).

In practice, the basic application of the normalized DFT is to *approximately* evaluate the spectrum of a real, continuous-time, nonperiodic signal $x(t)$. The signal $x(t)$ might be an electric field, voltage, current, etc. In numerical applications, we can deal only with the values of the signal at a finite number of discrete time instants.

This application of the DFT can be introduced in two ways. One way is to deal with the samples of the original continuous-time signal and the other way is to replace the original signal by a discrete-time signal. In both cases, we assume that the signal is almost time-limited to the interval $t \in [0, T)$.

Following the first approach, we take the samples (signal values) at N equispaced time instants, $t_n = n\Delta t$, $n = 0, 1, \dots, N-1$, i.e., we take $x_n = x(n\Delta t)$. We approximate the Fourier integral of $x(t)$ by a sum of “rectangles”, i.e., $\int_{-\infty}^{+\infty} x(t) e^{-2\pi jft} dt \approx \int_0^T x(t) e^{-2\pi jft} dt \approx \sum_{n=0}^{N-1} x(n\Delta t) e^{-2\pi jfn\Delta t} \Delta t$. We further assume that the spectrum of $x(t)$, $X(f)$, is almost frequency-limited to the interval $f \in \left[0, \frac{N}{2T}\right)$ and we consider this

spectrum only at discrete frequencies $f_k = k\Delta f = \frac{k}{T}$, $k = 0, 1, \dots, N/2-1$ (for N even). Knowing that the spectrum has a conjugate symmetry, we thus effectively consider N discrete values of the spectrum. Since

$f_k n\Delta t = \frac{nk}{N}$, we obtain $X(k\Delta f) \approx \Delta t \sum_{n=0}^{N-1} x(n\Delta t) e^{-2\pi j \frac{kn}{N}}$. This sum is the normalized DFT, so that

$X(k\Delta f) \approx \Delta t X_k$. Note that to obtain a proper approximation of the spectrum, we need to perform the multiplication by Δt .

Using the normalized IDFT, we obtain the values x_n in a similar way as $x(n\Delta t) \approx \Delta f \sum_{k=0}^{N-1} X_k e^{2\pi j \frac{nk}{N}}$.

Hence, $x(n\Delta t) \approx N\Delta f x_n$. Note that $N\Delta t\Delta f = 1$, so that this product is absorbed in the sequence of the direct and inverse DFT¹.

Assuming that N is even, the spectral components $X_0, X_1, \dots, X_{N/2-1}$ approximate the values of the spectrum $X(f)$ of the signal $x(t)$ at a set of discrete frequencies, i.e., $X_k = \frac{1}{\Delta t} X(k\Delta f)$, $n = 0, 1, \dots, N/2 - 1$.

According to the second approach to using the DFT to approximately evaluate the spectrum of the signal $x(t)$, we replace the continuous-time signal $x(t)$ by the discrete-time signal $x_{dt}(t) = x_{\delta t}(t)\Delta t$, where $x_{\delta t}(t)$ is given by (1). The need for multiplication by Δt can be justified in two ways. First, the unit for the delta-function $\delta(t)$ is s^{-1} , so that we have to restore the original unit for the signal $x(t)$. Second, we want $x(t)$ and $x_{dt}(t)$ to have approximately identical spectra, so that $x(t)$ and $x_{dt}(t)$ should have practically equal integrals² over any interval whose length is Δt . Following this approach, upon evaluating the Fourier integral, we again obtain the spectral samples to be $X(k\Delta f) \approx \Delta t X_k$.

In conclusion to this section, we point out that the DFT is an *exact* transform that maps a periodic sequence of impulses in the temporal domain into a periodic sequence of impulses in the spectral domain. However, when used to analyze a continuous-time signal (or a function whose temporal samples are known), the DFT only *approximately* evaluates spectral samples of such a signal. Similarly, the IDFT only approximately evaluates temporal samples of a function whose spectral samples are known. Thereby, we perform discretization both in the time domain and in the frequency domain. Hence, by applying the DFT, we *always* introduce an aliasing error because a continuous-time function cannot be limited both in the time domain and in the frequency domain. However, if we know that the function under consideration is *practically* limited to the time interval $(0, t_{\max})$ and also *practically* limited to the frequency range $(0, f_{\max})$, the application of the DFT/IDFT yields useful results.

¹ Some FFT algorithms use identical formulas for the direct and inverse FFT, apart for a sign change in the exponent. In such cases, the inverse DFT does not include the division by N , so that $x(n\Delta t) \approx \Delta f x_n$.

² Note that $\int_{-\varepsilon}^{\varepsilon} \delta(t) dt = 1$ for any $\varepsilon > 0$.

Care should also be taken when applying the DFT to the analysis of high-frequency electromagnetic problems, which always involve a delay. If the delay exceeds the period T and/or if the response does not settle down to zero fast enough, the response from one time window will penetrate into the subsequent time window, which will appear as a wrap-around of the response. A particular example where this periodicity causes trouble is the evaluation of the step response (the response to the Heaviside function). When applying the DFT, the Heaviside function must be replaced by a rectangular pulse, which jumps from 0 to 1 at the beginning of the time window and returns to zero around the middle of the same time window. The duration of the time window must be sufficient to allow the response to practically vanish within this window.

3. Temporal Leakage

The simplest, yet illustrative case where one can get acquainted with the temporal leakage is a delay line. Such a line can be a model of an ideal matched transmission line. If the line is excited by an impulse located at $t=0$, i.e., by $\delta(t)$, and if the delay is τ , the signal at the output of the line is given by $\delta(t-\tau)$. The objective is to evaluate this response using the normalized DFT. Since it is assumed that the impulse is located at $t=0$, we have $x_0=1$, $x_n=0$, $n=1, \dots, N-1$. We assume that $0 < \tau < (N-1)\Delta t$. Applying (8) yields the frequency-domain samples, $X_k=1$, $k=0, 1, \dots, N-1$. Next, the delay is expressed as $\tau = p\Delta t$ ($0 < p < N-1$) and this delay is simulated in the spectral domain by multiplying X_k by $\exp(-2\pi jkp/N)$, $k=0, \dots, N/2-1$. (This simulation mimics the analysis of an electromagnetic system or a circuit in the frequency domain.) The sample $X_{N/2}$ is peculiar because it must remain purely real. Hence, $X_{N/2}$ is multiplied only by $\text{Re}\{\exp(-\pi j p)\}$. The remaining samples, for $k=N/2+1, \dots, N-1$, are filled according to (9). Thereafter, the inverse normalized DFT (8b) is applied.

If p is an integer, a clean response is obtained using MATLAB [14], as shown in Fig. 1 for $p=150$. If this is not the case (e.g., $p=300.5$), the response contains oscillations (temporal leakage).

The temporal leakage can be explained by analytically evaluating the sum in (8b). Due to the conjugate symmetry in the spectral domain, one can write

$$x_n = \frac{1}{N} \left[1 + 2 \text{Re} \left\{ \sum_{k=1}^{\frac{N}{2}-1} e^{-\frac{2\pi j}{N}kp} e^{\frac{2\pi j}{N}kn} \right\} + \text{Re} \left\{ e^{\pi j(n-p)} \right\} \right]. \quad (10)$$

After summing the series in (10) and some manipulations, given in the Appendix, the result becomes

$$x_n = \frac{1}{N} \frac{\sin N\pi\alpha}{\tan \pi\alpha}, \quad (11)$$

where $\alpha = \frac{n-p}{N}$. Considering x_n as a function of α , it has a global maximum for $\alpha = 0$. This maximum is 1.

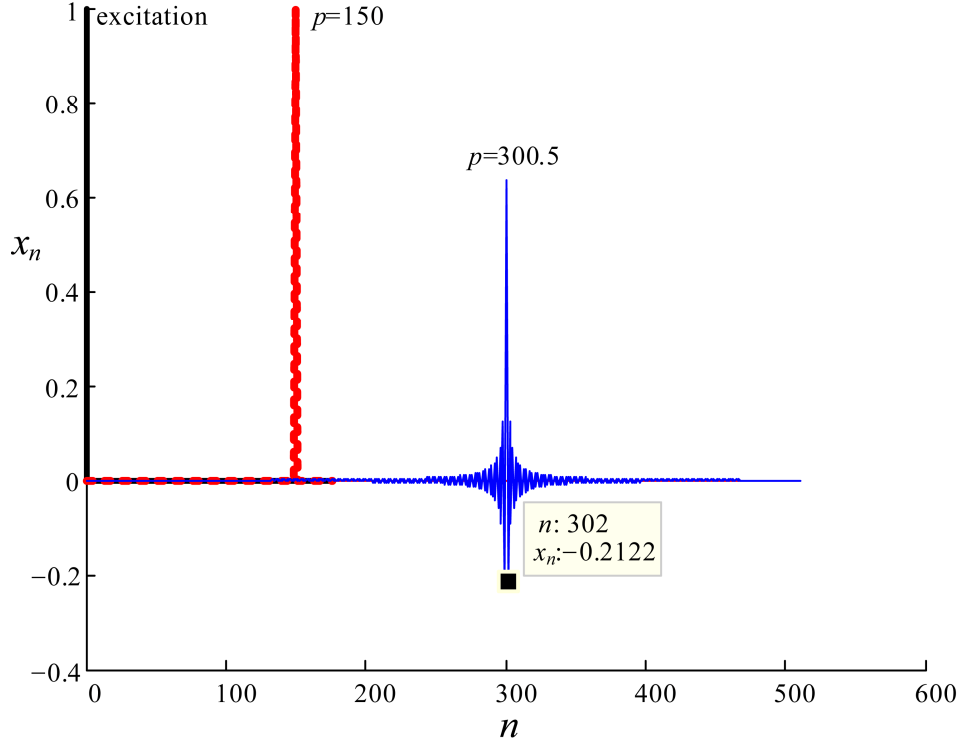


Fig. 1. Impulse excitation of a delay line and computed response (for $N = 512$) when $p = 150$ and $p = 300.5$.

However, p is an arbitrary given constant, whereas n is an integer. Hence, the global maximum can be attained only if p is also an integer, when the maximum occurs for $n = p$ ($x_p = 1$). In that case, all other samples are $x_n = 0$, $n = 0, \dots, N-1, n \neq p$, and a clean response is obtained, which is an impulse delayed for $\tau = p\Delta t$ after the excitation. If p is not an integer, the temporal leakage occurs. When $\alpha \ll 1$, i.e., in the vicinity of the delayed impulse, $\tan \pi\alpha \approx \pi\alpha$, so that

$$x_n \approx \frac{\sin N\pi\alpha}{N\pi\alpha} = \frac{\sin \pi(n-p)}{\pi(n-p)} = \text{sinc}(n-p). \quad (12)$$

The largest sample is the one whose index n is closest to p , but now $x_n < 1$. The largest leakage occurs if $p = m + 0.5$, where m is an integer. In that case, there are two largest samples, whose value is,

approximately, $\frac{2}{\pi} \approx 0.6366$. They are surrounded by two negative samples whose value is, approximately,

$$-\frac{2}{3\pi} \approx -0.2122, \text{ which can be verified in Fig. 1.}$$

The temporal leakage can also be explained in the following way. Let us consider the sequence (8b). If we want to delay this sequence for τ , all spectral components X_k , $k \in (-\infty, +\infty)$, must be multiplied by $\exp(-2\pi j f \tau)$. This multiplication modifies only the phase of X_k (Fig. 2), by reducing it by $2\pi f \tau$, which is plotted by the line denoted “natural”. However, in the general case, the resulting spectral components do not form a periodic sequence any more.

When we apply the DFT to evaluate the delay, we modify the phases of only the samples for $k = 0, \dots, N-1$, which belong to the basic spectral interval. (In Fig. 2, it is assumed that $N = 8$.) This phase shift is denoted by “DFT basic interval”. Thereafter, we periodically repeat the samples from this basic interval. Consequently, the phase shift is periodically repeated as denoted in Fig. 2 by “DFT periodically repeated”. Note that the phase shift of the samples for $k = -N/2 + 1, \dots, 0, \dots, N/2 - 1$ coincides with the natural phase shift.

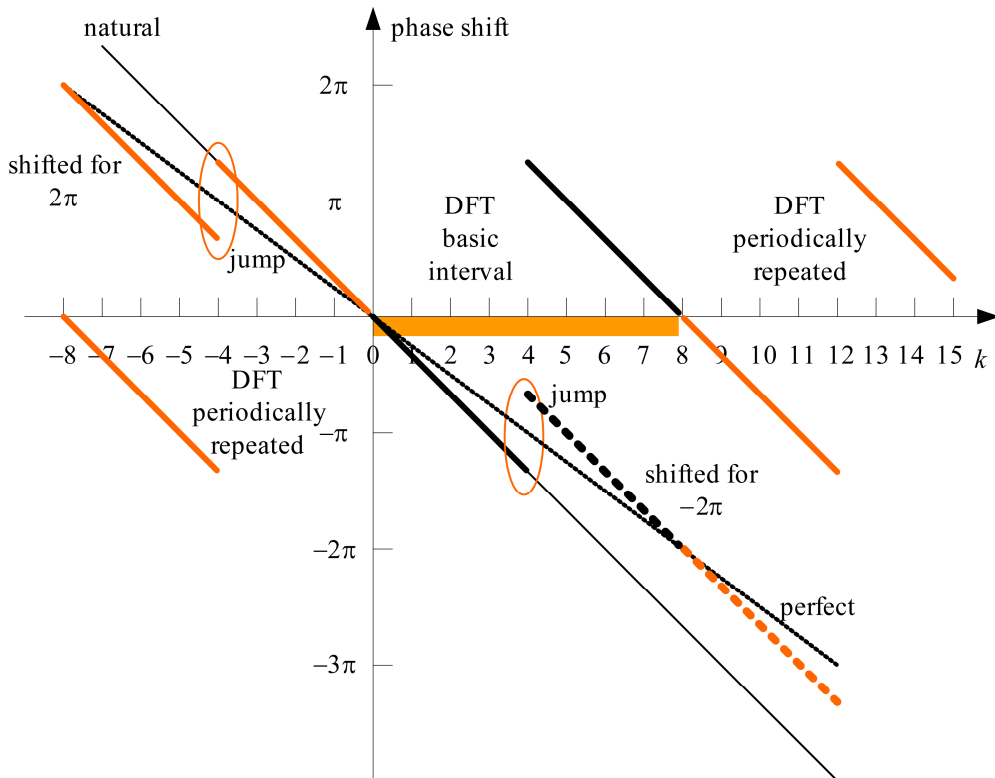


Fig. 2. Illustration of phase shifting when using DFT, which causes the temporal leakage.

Modifying the phase shift by an integer multiple of 2π does not change anything. Hence, we can try to overlap the DFT phase shift with the natural phase shift. (In the example shown in Fig. 2, the attempted shift is 2π , viz. -2π .) In the general case, the overlapping will not be possible and phase jumps would occur, as illustrated in Fig. 2. These jumps are the sources of the temporal leakage.

The only exceptions are cases when the natural phase shift at the sample N is an integer multiple of 2π (i.e., the delay τ is an integer multiple of Δt). In that case, the result obtained using the DFT exhibits a perfect delay. An example is the natural delay labeled “perfect” in Fig. 2.

4. Examples

As the first example in this section, Fig. 3 shows the response of a delay line to a rectangular pulse whose width is $50\Delta t$. The temporal leakage occurs around the pulse edges if the delay is not an integer multiple of Δt . In the response for $p = 300.5$, interference occurs between the ringings generated at the two transients, due to a small pulse width. If the pulse is sufficiently wide, the interference would be negligible. The maximal overshoots and undershoots occur when $p \approx m + 0.4$ or $p \approx m + 0.6$, and they amount to about 14% of the edge height. Note that the oscillations associated with the Gibbs phenomenon are given in terms of the sine integral function [15]. The resulting undershoots and overshoots at the transients would be about 9% of the edge height, i.e., smaller than those associated with the worst-case temporal leakage. The temporal leakage and the Gibbs phenomenon look similar, but they have different causes. The temporal leakage arises due to the discretization of a continuous signal, while the Gibbs effect arises due to limiting the bandwidth of the signal.

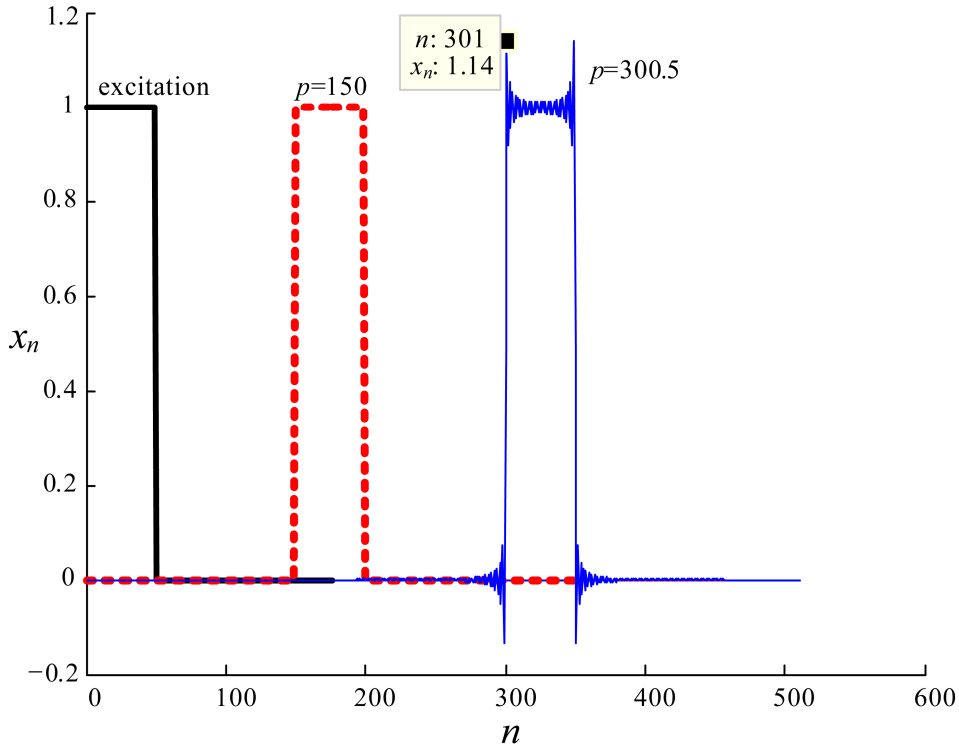


Fig. 3. Rectangular-pulse excitation of a delay line and computed response (for $N = 512$) when $p = 150$ and $p = 300.5$.

As the next example, we consider two wire antennas, separated by a distance of 2.1 m. The measured and simulated structure consists of a 225 mm long folded dipole, which acts as a transmitting antenna (Tx), and eight 80 mm long monopoles placed along the diagonal of an $1\text{m} \times 1\text{m}$ aluminum plate (Fig. 4). The first dipole acts as the receiving antenna (Rx), while the other 7 monopoles are terminated in $50\ \Omega$ loads [16]. The response was obtained by calculating the scattering parameter s_{21} using WIPL-D [3] and by measuring s_{21} (in the frequency domain) using a vector network analyzer and performing the IDFT. Fig. 5a shows the impulse response. The noncausal ringing caused by the temporal leakage (for $t < 7.1\text{ ns}$) is significantly reduced if the separation between the antennas is increased by just 25 mm (Fig. 5b) since this increase accidentally introduces a proper additional time delay and the corresponding phase shift.

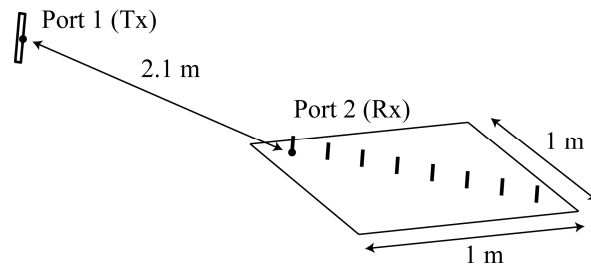
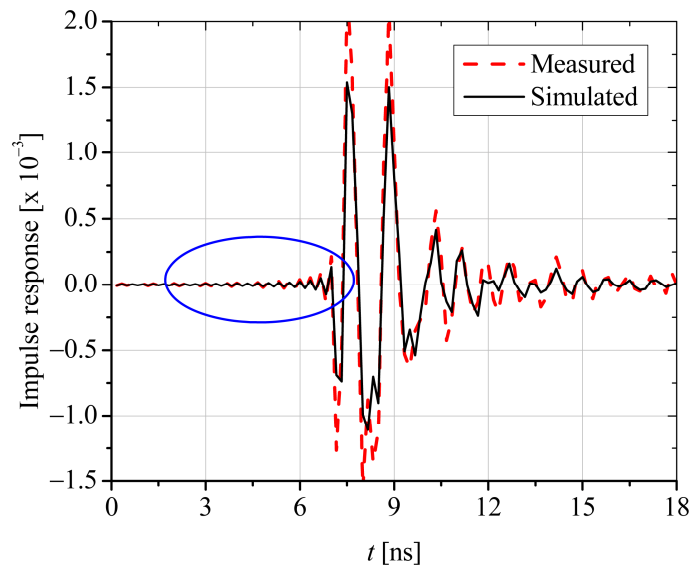
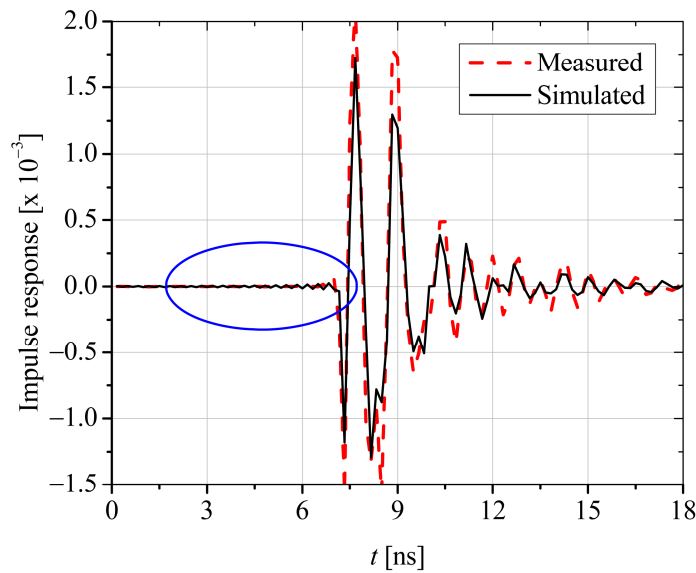


Fig. 4. Analyzed system with two antennas 2.1 m apart.



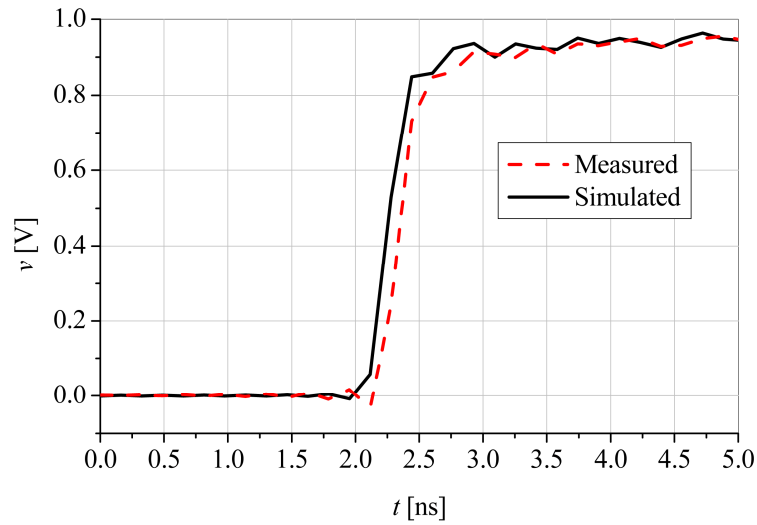
(a)



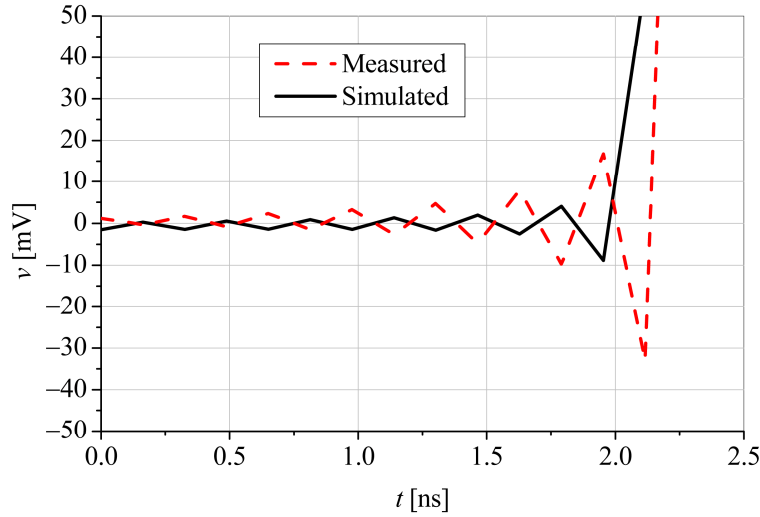
(b)

Fig. 5. (a) Impulse response of two antennas shown in Fig. 4 and (b) the response when the distance between the antennas is increased by 25 mm.

Finally, Fig. 6a shows the measured and simulated step response of a differential-mode fast digital-signal link. The link encompasses three multilayer printed-circuit boards and corresponding connectors. The simulated response was computed in the frequency domain using the model of the dielectric parameters [17] along with the model of the per-unit-length resistance and inductance [18], which guarantee a causal response. The latter model includes the edge effect, the proximity effect, the skin effect, and the effect of surface roughness. The model of the link also includes discontinuities at the connectors. First, the impulse response was evaluated using the IDFT of the scattering parameter s_{21} (involving frequency samples up to about 3 GHz), followed by a convolution to obtain the step response. Even after the convolution (which introduces smoothing), oscillations due to the temporal leakage persist in the response (Fig. 6b). The period of the oscillations equals twice the time step used in computations. The oscillations are clearly visible before the propagated step occurs. Thereafter, they are blended with oscillations due to multiple reflections on the link.



(a)



(b)

Fig. 6. (a) Step response of a fast digital-signal link and (b) zoom-in showing ringing due to temporal leakage.

By the above examples, we have demonstrated that the temporal leakage appears in results of numerical simulations and in measurements using vector network analyzers (which is true both if the analyzer has a built-in time-domain option and if the IDFT of the scattering parameters is performed externally).

The effects of the temporal leakage are artifacts in the time-domain response, which occur around fast transitions of the response. The artifacts are quasi-oscillatory, their period equals twice the time step,

and their amplitudes decay slowly away from the transitions. The oscillations occur not only after a transition, but also prior to it, so that an apparently non-causal response of a causal system is obtained.

In the worst-case scenario, the maximal effect of the temporal leakage can be as high as 21% of the impulse response (Fig. 1) and 14% of the step response or the pulse response (Fig. 3) for low-loss wideband systems (such as a simple transmission line). In other practical cases, however, the effect of the temporal leakage is usually smaller (Figs. 5 and 6), depending on the bandwidth of the system and the spectrum of the time-domain excitation.

The temporal leakage is less pronounced in systems with dispersion (e.g., a lossy transmission line) because sharp transitions cannot occur in such cases. Furthermore, the temporal leakage can be kept low by shaping the excitation functions appropriately, e.g., by applying a Gaussian pulse, which is often used to find figures of merit for time-domain radiators [19, 20]. In such cases, the amplitudes of the oscillations due to the temporal leakage are on the order of a few percent of the actual response or even less, so that the temporal leakage is often blended with oscillations due to other causes. Note, however, that in some cases the impulse response is indispensable (e.g., when evaluating responses by convolution and when modeling nonlinear systems [21]), when the response to Dirac's delta-function cannot be replaced by the response to the Gaussian pulse.

The temporal leakage can be practically eliminated in a system whose response is affected by a single physical time delay (e.g., a single-path transmission between two matched antennas). In such a case, the number of frequencies and/or the frequency step at which the response is measured or computed may be changed with the aim to make this delay equal to an integer multiple of the time step. For example, we can freeze the frequency step and change the upper frequency used in the computations by changing the total number of samples. A peculiarity of this procedure is that the temporal leakage will periodically decrease and increase as the number of samples is changed. However, in the general case, i.e., when the system is characterized by two or more non-commensurate time delays (e.g., a multipath transmission between two antennas or a microwave circuit with several reflection points), the temporal leakage will always be present.

5. Conclusions

This paper explained and demonstrated the temporal leakage. First, we mathematically explained why the temporal leakage occurs. We also showed that when applying the discrete Fourier transform, an apparently noncausal response can be obtained in the time domain, in spite of careful modeling in the frequency domain. Finally, we presented some typical cases where the temporal leakage occurs in the electromagnetic analysis as well as in measurements.

6. Acknowledgments

The authors thank their student Mr. Djordje Mirković for providing motivation for the paper and meticulous reading.

This work was supported in part by the Serbian Ministry of Education and Science under Grant TR32005 and by the COST action IC1102 VISTA.

7. References

- [1] B. M. Kolundžija and A. R. Djordjević, *Electromagnetic Modeling of Composite Metallic and Dielectric Structures*, Norwood, MA, Artech House, 2002.
- [2] HFSS 13.0, ANSYS, Inc., *3D Full-wave Electromagnetic Field Simulation*, <http://www.ansoft.com/products/hf/hfss/>.
- [3] WIPL-D Pro 8.0, 3D Electromagnetic Solver, <http://www.wipl-d.com>.
- [4] D. I. Olćan, M. M. Nikolić, B. M. Kolundžija, and A. R. Djordjević, "Time-Domain Response of 3-D Structures Calculated Using WIPL-D," *Proceedings of ACES 2007*, Verona, Italy, March 2007, pp. 525-531.
- [5] M. M. Potrebić, D. V. Tošić, and P. V. Pejović, "Understanding Computation of Impulse Response in Microwave Software Tools," *IEEE Transactions on Education*, **EDU-53**, 4, November 2010, pp. 547-555.
- [6] M. S. O'Brien and S. M. Kramer, "Temporal Leakage and Its Effects on Resolution in Deconvolution of Ultrasonic Signals," in *Review of Progress in Quantitative Nondestructive Evaluation*, **11A**; Proceedings of 18th Annual Review, Brunswick, ME, July 28-August 2, 1991, pp. 911-918.
- [7] P. M. A. Warwick, *Analysis and Application of the Spectral Warping Transform to Digital Signal Processing*, Thesis, Institute of Information Sciences and Technology, Massey University, Palmerston North, New Zealand, 2007.
- [8] M. R. Coble, G. C. Papen, and C. S. Gardner, "Computing Two-Dimensional Unambiguous Horizontal Wavenumber Spectra from OH Airglow Images," *IEEE Transactions on Geoscience and Remote Sensing*, **36**, 2, March 1998, pp. 368-382.
- [9] G. Yao and S.-I. Chu, "Strong Field Effects in Above-Threshold Detachment of a Model Negative Ion," *Journal of Physics B: Atomic Molecular and Optical Physics*, **25**, 2, January 1992, pp. 363-376.
- [10] S. Zegenhagen, A. Werner, A. Weller, and T. Klinger, "Analysis of Alfvén Eigenmodes in Stellarators Using non-Evenly Spaced Probes," *Plasma Physics and Controlled Fusion*, **48**, pp. 1333-1346, 2006.

- [11] J. D. Cameron, *Stall Inception in a High-Speed Axial Compressor*, Ph.D. Dissertation, University of Notre Dame, Indiana, USA, 2007.
- [12] W. Y. Yang, T. G. Chang, I. H. Song, Y. S. Cho, J. Heo, W. G. Jeon, J. W. Lee, and J. K. Kim, *Signals and Systems with MATLAB*, Heidelberg, Springer, 2009.
- [13] D. Havelock, S. Kuwano, and M. Vorländer, *Handbook of Signal Processing in Acoustics*, Volume 1, New York, Springer, 2008.
- [14] MATLAB, The MathWorks, Inc., <http://www.mathworks.com/>.
- [15] D. W. Kammler, *A First Course in Fourier Analysis*, New York, Cambridge University Press, 2007, pp. 44-45.
- [16] M. M. Nikolić, A. Nehorai, and A. R. Djordjević, “Biologically Inspired Sensing on UAV Platform,” *Proceedings of 2011 IEEE International Symposium on Antennas and Propagation and USNC/URSI Meeting (AP-S 2011)*, July 3-8, 2011, Spokane, WA, USA, pp. 1537-1540.
- [17] A. R. Djordjević, R. M. Biljić, V. D. Likar-Smiljanić, and T. K. Sarkar, “Wideband Frequency-Domain Characterization of FR-4 and Time-Domain Causality,” *IEEE Transactions on Electromagnetic Compatibility*, **EMC-43**, 4, November 2001, pp. 662-667.
- [18] I. Jovanović, *Ultrafast Digital-Signal Interconnects on Printed-Circuit Boards*, M.Sc. Thesis, University of Belgrade, School of Electrical Engineering, Belgrade, Serbia, 2010.
- [19] C. E. Baum, E. G. Farr, and D. V. Giri, “Review of Impulse-Radiating Antennas,” in W. R. Stone (ed.), *Review of Radio Science 1996-1999*, Oxford University Press, 1999, ch. 16, pp. 403-438.
- [20] D. Ghosh, A. De, M. C. Taylor, T. Sarkar, C. Wicks, and E. L. Mokole, “Transmission and Reception by Ultra-Wideband (UWB) Antennas,” *IEEE Antennas and Propagation Magazine*, **48**, 5, October 2006, pp. 67-99.
- [21] A. R. Djordjević and T. K. Sarkar, “Transient Analysis of Electromagnetic Systems with Multiple Lumped Nonlinear Loads,” *IEEE Transactions on Antennas and Propagation*, **AP-33**, 5, May 1985, pp. 533-539.

Appendix

We derive here equation (11). We start from (10) and sum the geometric series as

$$\sum_{k=1}^{\frac{N}{2}-1} e^{-\frac{2\pi j}{N}kp} e^{\frac{2\pi j}{N}kn} = e^{\frac{2\pi j}{N}(n-p)} \frac{e^{\frac{2\pi j}{N}(\frac{N}{2}-1)(n-p)} - 1}{e^{\frac{2\pi j}{N}(n-p)} - 1}. \text{ We extract from the numerator the term } e^{\frac{\pi j}{N}(\frac{N}{2}-1)(n-p)} \text{ leaving}$$

$$e^{\frac{\pi j}{N}(\frac{N}{2}-1)(n-p)} - e^{-\frac{\pi j}{N}(\frac{N}{2}-1)(n-p)} = 2j \sin\left(\frac{N}{2}-1\right) \frac{\pi(n-p)}{N}.$$

Similarly, from the denominator we extract the term $e^{\frac{\pi j}{N}(n-p)}$ leaving $e^{\frac{\pi j}{N}(n-p)} - e^{-\frac{\pi j}{N}(n-p)} = 2j \sin \frac{\pi(n-p)}{N}$.

Hence, the sum becomes $\sum_{k=1}^{\frac{N}{2}-1} e^{-\frac{2\pi j}{N}kp} e^{\frac{2\pi j}{N}kn} = e^{\frac{\pi j}{N}(n-p)} \frac{\sin\left(\frac{N}{2}-1\right) \frac{\pi(n-p)}{N}}{\sin \frac{\pi(n-p)}{N}}$. Substituting this sum into (10) and

setting $\frac{n-p}{N} = \alpha$ yields $x_n = \frac{1}{N} \left[1 + 2 \cos \frac{N}{2} \pi \alpha \frac{\sin\left(\frac{N}{2}-1\right) \pi \alpha}{\sin \pi \alpha} + \cos N \pi \alpha \right]$.

Finally, using the trigonometric identities $1 + \cos N \pi \alpha = 2 \cos^2 \frac{N \pi \alpha}{2}$ and

$$\sin\left(\frac{N}{2}-1\right) \pi \alpha = \sin \frac{N}{2} \pi \alpha \cos \pi \alpha - \cos \frac{N}{2} \pi \alpha \sin \pi \alpha, \text{ equation (11) is obtained.}$$



Antonije R. Djordjević was born in Belgrade, Serbia, on April 28, 1952. He received the B.Sc., M.Sc., and Ph.D. degrees from the School of Electrical Engineering, University of Belgrade, in 1975, 1977, and 1979, respectively. In 1975, he joined the School of Electrical Engineering, University of Belgrade, as a Teaching Assistant. He was promoted to an Assistant Professor, Associate Professor, and Professor, in 1982, 1988, and 1993, respectively. In 1983, he was a Visiting Associate Professor at Rochester Institute of Technology, Rochester, NY. Since 1992, he has been an Adjunct Scholar with Syracuse University, Syracuse, NY. In 1997, he became a Corresponding Member of the Serbian Academy of Sciences and Arts, and he became a full member in 2006. His main area of interest is numerical electromagnetics, in particular applied to fast digital signal interconnects, wire and surface antennas, microwave passive circuits, and electromagnetic-compatibility problems.



Dejan V. Tošić was born in Belgrade, Serbia, in 1957. He received the B.Sc. (1980), M.Sc. (1986), and Ph.D. (1996) degrees from the School of Electrical Engineering, University of Belgrade, Serbia. He is currently a Full Professor with the School of Electrical Engineering, University of Belgrade. He is a coauthor of the book *Filter Design for Signal Processing Using MATLAB and Mathematica* (Prentice-Hall, 2001, translated in Chinese by PHEI, Beijing, China, 2004), a coauthor of the book *WIPL-D Microwave: Circuit and 3D EM Simulation for RF & Microwave Applications* (Artech House, 2005), and a coauthor of *SchematicSolver*, a software package for symbolic and numeric analysis, processing, and design of analog and digital systems (<http://www.wolfram.com/products/applications/schematicsolver/>). His research interests include symbolic computation and signal processing, RF and microwave filter design, and design of passive microwave circuits.



Alenka G. Zajić (S'99-M'08) received her B.Sc. and M.Sc. degrees from the School of Electrical Engineering, University of Belgrade, in 2001 and 2003, respectively. She received her Ph.D. degree in Electrical and Computer Engineering from the Georgia Institute of Technology in 2008. In 2010, she joined the School of Computer Science, Georgia Institute of Technology, where is Visiting Assistant Professor. Her research interests are in wireless communications and applied electromagnetics. Dr. Zajić received the Best Paper Award at ICT 2008, the Best Student Paper Award at WCNC 2007, and was also the recipient of the Dan Noble Fellowship in 2004, awarded by Motorola Inc. and IEEE Vehicular Technology Society for quality impact in the area of vehicular technology.



Marija M. Nikolić received the B.Sc., M.Sc., and Ph.D. degrees from University of Belgrade in 2000, 2003, and 2007, respectively. In 2001, she joined the School of Electrical Engineering, University of Belgrade as a Teaching Assistant. In 2008 she was promoted to an Assistant Professor. In 2011, she obtained the Ph.D. degree in electrical engineering from Washington University in St. Louis, USA. She is interested in inverse scattering, array processing, and antenna analysis and design.



Dragan I. Olćan (S'05-M'09) is an Assistant Professor at the School of Electrical Engineering, University of Belgrade, Serbia, where he received his B.Sc., M.Sc., and Ph.D. degrees in 2001, 2004, and 2008, respectively. He is a coauthor of two commercial electromagnetic software codes, five journal papers,

about forty conference papers, and four university textbooks. His main research interests are: diakoptic approach to numerical electromagnetic analysis, optimization algorithms applied to electromagnetic design, time-domain electromagnetic analysis, and applied electromagnetics.



Izabela D. Jovanović was born in Belgrade, Serbia, in 1972. She received her B.Sc. and M.Sc. degrees from the School of Electrical Engineering, University of Belgrade, in 1998 and 2010, respectively. From 1998 until 2004, she worked as R&D engineer at the Institute for Microwave Techniques and Electronics (IMTEL) in Belgrade. Since 2004, she has been with “Telekom Srbija” in Belgrade as leading engineer.